Mode transition in radio-frequency atmospheric argon discharges with and without dielectric barriers

J. J. Shi and M. G. Kong[a)]

Department of Electronic and Electrical Engineering, Loughborough University, Loughborough, Leicestershire LE11 3TU, United Kingdom

In this letter, basic characteristics of glow modes and their mode transition are studied for radio-frequency (rf) atmospheric argon discharges with bare and dielectrically insulated electrodes. Through input power control, large-volume rf atmospheric argon discharges with bare electrodes are achieved in the α mode via an abrupt transition from a constricted γ mode, whereas dielectrically insulated electrodes result in large argon discharges in both the α and γ modes with gradual mode transition. Current dependence of the 750 nm line intensity and of the gas temperature are shown to capture clearly the signature of mode transition. © *2007 American Institute of Physics*.
[DOI: 10.1063/1.2711413]

Research in atmospheric-pressure glow discharges (APGDs) has recently attracted considerable interest, largely because of their immense application potential.[1,2] This is further fuelled by the intriguing similarity and contrast in their underpinning physics to low-pressure glow discharges, despite of the fact that the two types of glow discharges operate in distinctively different collisional regimes.[3] For many applications requiring treatment of extensive surface areas, large-scale APGDs are critical but difficult to achieve due to their tendency for the glow-to-arc transition. While this can be addressed by using helium as the working gas, it is desirable to realize APGD applications with less expensive gases such as argon and nitrogen.[4] Using radio-frequency (rf) excitation at which gas breakdown voltage is low[5] and plasma stability is robust,[6] large-area Ar rf APGDs have been achieved with unconventional electrodes such as microstructured electrodes,[7] multiple electrodes,[8] and microslot electrodes.[9] Recently, dielectric insulation of electrodes is also found beneficial.[10,11] By increasing the power input after gas breakdown, dielectrically insulated electrodes lead to large-area homogenous Ar APGD, whereas bare electrodes tend to evolve the argon discharge directly into constricted plasma. However, little is known of the underpinning physics. In this letter, we present an experimental study of fundamental characteristics of glow modes and their mode transition in Ar rf atmospheric glow discharges with and without dielectric barriers.

The argon rf atmospheric discharge considered in this study was generated between two parallel stainless-steel round plates with an identical diameter of 20 mm. Each electrode was covered with a square ceramic sheet of 25×25 mm^2 in surface area and 0.5 mm in thickness. The ceramic sheets have a relative permittivity of 9.0. The electrode unit had a gas gap of 2.0 mm and was enclosed in a Perspex box with an argon flow of 5 l/min at 760 torr. The generated plasma is essentially an rf dielectric-barrier discharge (DBD) in atmospheric argon. To distinguish it from conventional atmospheric discharges generated between two bare electrodes, the latter is referred to as rf APGD. A comparable rf

APGD was produced using the same electrode unit but without the ceramic sheets and with the gas gap fixed at 2.0 mm. For both the rf DBD and the rf APGD, one electrode was powered, via a homemade impedance matching network, by a radio-frequency power source in which a 13.56 MHz sinusoidal signal was generated by a function generator (Tektronix AFG 3102) and amplified by a power amplifier (AR 150A100B). The discharge current and the applied voltage were measured by a wideband current probe (Tektronix P6021) and a wideband voltage probe (Tektronix P6015A), and their wave forms were recorded on a digital oscilloscope (Tektronix TDS 3034B). An intensified charge-coupled device camera (Andor i-Star DH720) was used to capture plasma images. Optical emission spectrum was obtained using a spectrometer system (Andor Shamrock) with a focal length of 0.3 m and a grating of 600 grooves/mm.

Figure 1 shows the current-voltage characteristics for the Ar rf APGD and the Ar rf DBD, for which gas breakdown
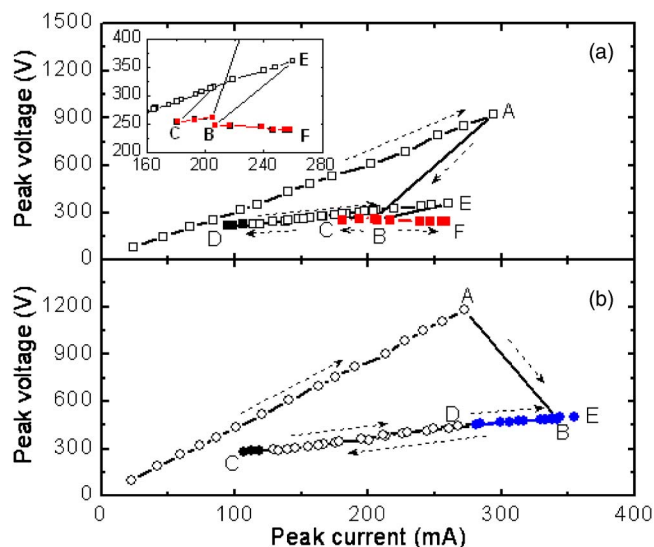
FIG. 1. (Color online) Current-voltage characteristics of (a) the Ar rf APGD with the inset showing an enlarged part of its current-voltage relationship and (b) the Ar rf DBD. Open markers indicate the α mode and the black solid markers indicate the normal glow mode. Red and blue solid markers indicate the constricted γ mode and the usual large-volume γ mode.

[a)]Author to whom correspondence should be addressed; electronic mail: m.g.kong@lboro.ac.uk

occurs at a peak applied voltage of V_p=925 and 1180 V, respectively. The larger breakdown voltage of the rf DBD is a result of its two dielectric barriers dividing into the applied voltage.[11] For both atmospheric argon discharges, the applied voltage undergoes a large reduction of more than 660 V immediately after the breakdown, distinctly different from rf glow discharges in atmospheric helium.[10,11] Subsequently, the Ar rf APGD evolved directly into a constricted plasma column of about 1 mm in diameter at point B in Fig. 1(a) image not shown) and further increase in the input rf power was found to be incapable of evolving the constricted plasma into a large-volume homogenous discharge. However, if instead the input power reduces from that at point B, an intriguing sequence of mode transition develops. Initially, the constricted plasma persists from point B to point C as indicated by red solid squares in Fig. 1(a). Then at point C, it expands abruptly to fill up the entire interelectrode space. The resulting homogeneous discharge is most likely to be an α mode,[12–16] judging by the lack of a clear sheath structure in its image (not shown) and by its positive differential conductivity shown in Fig. 1(a)[13,14,16] With further reduction of the input power, the rf APGD remains homogenous until point D after which it is extinguished. Interestingly as the rf APGD moves toward its extinction point, the electrode area it covers becomes progressively smaller in a fashion that resembles the transition from the abnormal to normal glow modes.

If the input rf power is increased at point D, the Ar rf APGD initially expands in its diameter evolving from the normal to abnormal glow modes before taking up the entire interelectrode space until point E where an abrupt transition into a constricted plasma occurs. Therefore, large-volume Ar rf APGDs in the α mode can be attained over a range of the peak current from 181.0 to 260.0 mA if the input rf power is decreased after gas breakdown and then increased at the plasma extinction point. This has not been observed before. After the transition from point E and with increasing input power, the constricted plasma remains constricted until point F where the power amplifier reaches its output limit. It is of interest to note that after transition from point E the Ar plasma recovers to point B in Fig. 1(a), the same point to which the discharge moves from gas breakdown. It is also worth noting the hysteretic trajectory of the rf APGD in its current-voltage characteristics of Fig. 1(a).

To illustrate the above sequence of mode transition, images of the Ar rf APGDs taken with 500 μs exposure time are shown in Fig. 2(a). Corresponding to point D immediately before plasma extinction in Fig. 1(a), the first image in Fig. 2(a) shows a homogeneous discharge that covers only part of the electrodes and is in the normal glow mode. The second image corresponds to point E in Fig. 1(a), exhibiting volumetric optical emission which is a characteristic of the α mode.[11,13,16] These were also confirmed by nanosecond imaging (image not shown). The case of the constricted plasma is shown in the third image of Fig. 2(a), typical of the Ar discharge from point B to either point C or point F in Fig. 1(a) marked with red solid squares). While not useful for applications, such constricted plasma is not an arc since it can persist for many tens of minutes. Close to the two electrodes, it has two bright thin layers, likely to be a negative glow and indicative of narrow sheaths.[11] Its characters are therefore that of the γ mode.[12–16] From the standpoint of the underpinning science and practical use, this constricted γ
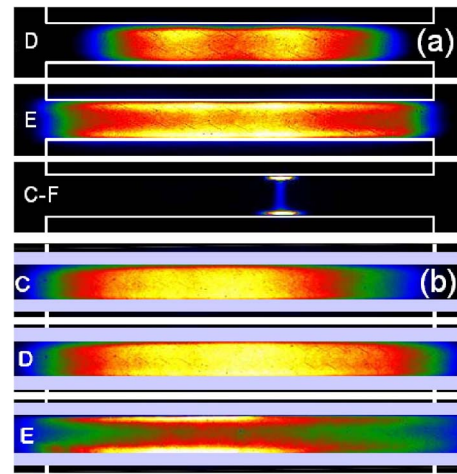

FIG. 2. (Color online) Plasma images of (a) the Ar rf APGD and (b) the Ar rf DBD. Letters on the left hand side of the images corresponds to the same letters in Fig. 1.

mode is different from the large-volume γ mode observed in rf DBD (Refs. 10 and 11) and microgap rf APGD.[16] Therefore, we refer the large-volume γ mode to as the γ mode and the constricted plasma to as being in the γ_c mode. With this reference, gas breakdown in the Ar rf APGD evolves it directly into the γ_c mode. Then with decreasing input power, the $\gamma_c-\alpha$ mode transition occurs immediately after point C in Fig. 1(a). If the input rf power is increased before plasma extinction at point D, the Ar rf APGD can remain in the α mode over a sizable range of the discharge current before undergoing an α-γ_c mode transition at point E.

Mode transition in the Ar rf DBD is simpler. Its appearance immediately after gas breakdown is volumetric and occupies the entire interelectrode space on a nanosecond scale (image not shown). This corresponds to point B in Fig. 1(b) at which the peak current is I_p=341.5 mA and V_p=487.6 V. If the input power is increased from this point onwards, the Ar rf DBD remains volumetric until the output limit of the power amplifier at point E in Fig. 1(b). Appearance of the rf DBD at point E is shown in the last image in Fig. 2(b), where one bright thin line is seen near each of the two electrodes suggesting the existence of the negative glow and a strong sheath region.[11–16] Combining with a highly localized optical emission, these suggest that the rf DBD is in the γ mode at point E.

If the input power is reduced instead at point B in Fig. 1(b), the rf DBD initially remains in its γ mode. Then its optical emission becomes increasingly less localized and gradually becomes volumetric at point D at which V_p=442.5 V and I_p=267.0 mA. This is illustrated in the second image of Fig. 2(b) where the plasma is clearly volumetric with no obvious sheath structure. In other words, the Ar rf DBD enters the α mode at point D through a gradual $\gamma-\alpha$ mode transition. With further reduction in the input rf power, its α mode character remains so until shortly before its extinction at point C in Fig. 1(b). Similar to the Ar rf APGD, the extinction point is preceded with an abnormal-normal mode transition that leads to the discharge covering only partially the electrodes, as illustrated by the first image in Fig. 2(b). If the input power is increased at point C, the Ar rf DBD develops in an exact reversal of the B-D-C route and experiences an $\alpha-\gamma$ mode transition, again at point D. The trajectory of the Ar rf DBD in the current-voltage character-
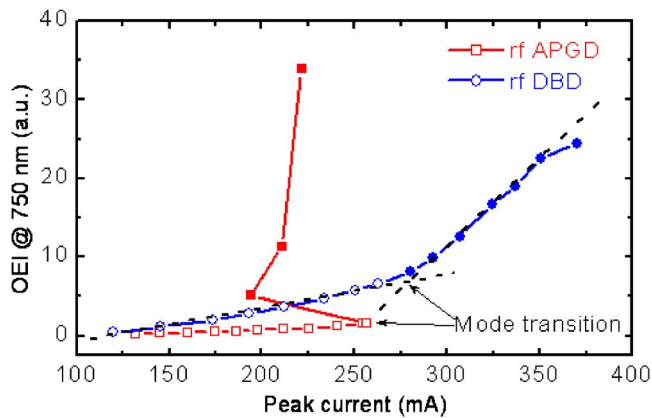
FIG. 3. (Color online) Current dependence of the optical emission intensity at 750 nm in the rf APGD and the rf DBD. Open markers indicate the α mode, whereas the red and blue solid markers indicate the γ_c and γ modes, respectively.
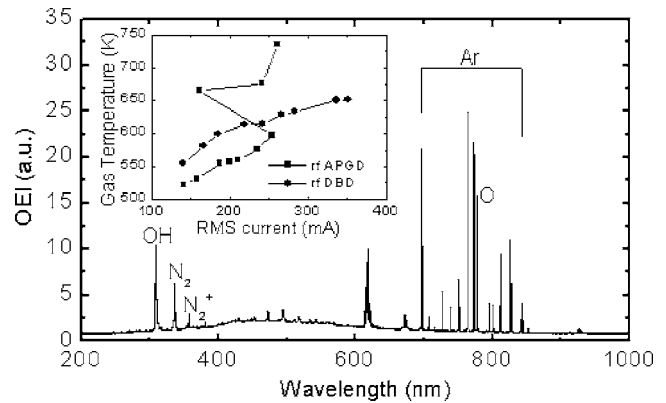

FIG. 4. Optical emission spectrum of the Ar rf DBD with the inset being the current dependence of gas temperature in the rf APGD and the rf DBD.

istics of Fig. 1(b) is independent of whether the input power increases or decreases.

Optical emission spectra from both the Ar rf APGD and the Ar rf DBD are dominated by argon lines with less intensive emission from various nitrogen, oxygen, and OH lines. Of particular interest is the 750 nm argon line that has been used as the signature of electrons in low-pressure argon glow discharges.[17] Given that the $\alpha - \gamma$ mode transition is directly associated with a step change in the electron density, the emission intensity at 750 nm is plotted as a function of the discharge current in Fig. 3. It is evident that the 750 nm line intensity in the rf APGD starts to increase significantly at $I_p = 256.5$ mA, corresponding to point E in Fig. 1(a). Its increase then occurs at a lower current of $I_p = 194.0$ mA, corresponding to point B in Fig. 1(a) and its subsequent growth is exponential. This suggests a substantial change in the electron density and an abrupt $\alpha - \gamma$ mode transition, consistent with the analyses of Figs. 1(a) and 2(a). In contrast, the $\alpha - \gamma$ mode transition in the Ar rf DBD occurs much more smoothly around $I_p = 279.1$ mA at which the slope of the 750 nm line intensity undergoes a small step change. This is consistent with the gradual change in the current-voltage characteristics and the plasma images of the Ar rf DBD.[18] The 750 nm line intensity is therefore an alternative indicator of mode transition in argon atmospheric glow discharges. Current dependence of the gas temperature also contains signature of mode transition. Estimated from the OH emission line at 307 nm with a finer grating of 2400 grooves/mm and using the LIFBASE software,[19] gas temperature is shown in Fig. 4 to increase abruptly after, $I_p = 254.0$ mA in the Ar rf APGD, whereas $I_p = 185.0$ mA is clearly a transition point in gas temperature of the Ar rf DBD. These are consistent with the evolution of the current-voltage relationship and plasma images.

In conclusion, large-volume Ar rf APGDs in the α mode have been achieved by reducing the input power immediately after gas breakdown before increasing it at the plasma extinction point. This power control was shown to accompany a hysteretic mode transition evolving from a $\gamma_c - \alpha$ transition to an $\alpha - \gamma_c$ transition. By contrast, large-volume Ar rf DBDs have been achieved both in the α and in the γ modes with little danger of plasma constriction. Mode transition is abrupt in the rf APGD and smooth in the rf DBD, as reflected in the current dependence of both the 750 nm line intensity and the gas temperature. The use of dielectric barriers seems to spatially suppress the occurrence of many plasma instabilities inherent in Ar rf APGD and as such achieve well-controlled dynamics in Ar rf DBD.

[1]H. Shirai, T. Kobayashi, and Y. Hasegawa, Appl. Phys. Lett. **87**, 143112 (2005).
[2]X. T. Deng, J. J. Shi, G. Shama, and M. G. Kong, Appl. Phys. Lett. **87**, 153901 (2005).
[3]U. Kogelschatz, Plasma Chem. Plasma Process. **23**, 1 (2003).
[4]N. Gherardi and F. Massines, IEEE Trans. Plasma Sci. **29**, 536 (2001).
[5]J. Park, I. Henins, H. W. Herrmann, and G. S. Selwyn, J. Appl. Phys. **89**, 15 (2001).
[6]J. J. Shi and M. G. Kong, Appl. Phys. Lett. **87**, 201501 (2005).
[7]K. H. Gericke, C. Gebner, and P. Scheffler, Vacuum **65**, 291 (2002).
[8]S. Y. Moon, J. W. Han, and W. Choe, Thin Solid Films **506-507**, 355 (2006).
[9]A. Rahman, A. P. Yalin, V. Surla, O. Stan, K. Hoshimiya, Z. Yu, E. Littlefield, and G. J. Collins, Plasma Sources Sci. Technol. **13**, 537 (2004).
[10]J. J. Shi, D. W. Liu, and M. G. Kong, Appl. Phys. Lett. **89**, 081502 (2006).
[11]J. J. Shi, D. W. Liu, and M. G. Kong, Appl. Phys. Lett. **90**, 031505 (2007).
[12]X. Yang, M. Moravej, G. R. Nowling, S. E. Babayan, J. Panelon, J. P. Chang, and R. F. Hicks, Plasma Sources Sci. Technol. **14**, 314 (2005).
[13]J. J. Shi and M. G. Kong, J. Appl. Phys. **97**, 023306 (2005).
[14]J. J. Shi and M. G. Kong, IEEE Trans. Plasma Sci. **33**, 624 (2005).
[15]S. Y. Moon, J. K. Rhee, D. B. Kim, and W. Choe, Phys. Plasmas **13**, 033502 (2006).
[16]J. J. Shi and M. G. Kong, Phys. Rev. Lett. **96**, 105009 (2006).
[17]P. P. Ray and P. Chaudhuri, Econ. Plann. **53**, 229 (2003).
[18]J. J. Shi, X. T. Deng, R. Hall, J. D. Punnett, and M. G. Kong, J. Appl. Phys. **94**, 6303 (2003).
[19]J. Luque and D. R. Crosley, SRI International Report No. MP 99–009 ⟨http://www.sri.com/psd/lifbase/⟩ (1999).